



Resveratrol Prevents the Cellular Damages Induced by Monocrotophos via PI3K Signaling Pathway in Human Cord Blood Mesenchymal Stem Cells

S. Jahan^{1,2} · D. Kumar^{1,2} · S. Singh^{1,2} · V. Kumar¹ · A. Srivastava¹ · A. Pandey¹ · C. S. Rajpurohit^{1,2} · V. K. Khanna^{1,2} · A. B. Pant^{1,2}

Received: 8 August 2017 / Accepted: 28 February 2018 / Published online: 10 March 2018

© Springer Science+Business Media, LLC, part of Springer Nature 2018

Abstract

The role of resveratrol (RV) as a neuroprotectant is well recognized, and cellular molecules involved in imparting the physiological effect have been well illustrated. However, some ambiguity still prevails as the specific receptor, and downstream signaling molecules are not yet clearly stated. So, we investigated the signaling pathway(s) involved in its cellular protection in the human umbilical cord blood mesenchymal stem cell (hUCB-MSC) derived neuronal cells. The mesenchymal stem cells were exposed to various concentrations (10, 100, 1000 μM) of monocrotophos (MCP), a known developmental neurotoxic organophosphate pesticide, for a period of 24 h. The MAPK signaling pathways (JNK, p38, and ERK) known to be associated with MCP-induced damages were also taken into consideration to identify the potential connection. The biological safe dose of RV (10 μM) shows a significant restoration in the MCP-induced alterations. Under the specific growth conditions, RV exposure was found to promote neuronal differentiation in the hUCB-MSCs. The exposure of cells to a specific pharmacological inhibitor (LY294002) of PI3K confirms the significant involvement of PI3K-mediated pathway in the ameliorative responses of RV against MCP exposure. Our data identifies the substantial role of RV in the restoration of MCP-induced cellular damages, thus proving to have a therapeutic potential against organophosphate pesticide-induced neurodegeneration.

Keywords Resveratrol · Monocrotophos · PI3K · Neuroprotection · Human umbilical cord blood mesenchymal stem cells

Introduction

The central nervous system (CNS) being a complex system of our body is particularly vulnerable to a large number of toxicants/xenobiotics persisting in the environment [1]. Worst affected is the developing phase of the nervous system which is highly prone to accumulating damages incurred due

to in utero exposure to certain toxicants that may eventually lead to neurodevelopmental anomalies. Neurotoxicants present in the surroundings can harm the brain cells/neurons beyond repair and are majorly responsible for neurodegenerative disorders [2]. These diseases are progressive in nature and incurable so far [3]. A number of drugs/chemicals have been linked with the incidence of such diseases which largely include inorganic metals, organometals, and several pesticides [4]. Organophosphate (OP) pesticides have emerged as a potent class of neurotoxicants. Residues and metabolites of OP have been identified in dietary products as well as in biological tissues raising concern regarding their neurotoxic burden [5]. OP targets the entire body; however, brain is the most vulnerable target for the induction of neurotoxicity that results in long-term neurobehavioral alterations [6].

Monocrotophos (MCP) is a well-known organophosphate insecticide. Its primary mechanism of action is its irreversible inhibition of acetylcholinesterase, an enzyme essential for nerve impulse transmission in the cholinergic neurons [7]. However, it also demonstrates its toxic effect via necrosis,

S. Jahan and D. Kumar are equal contributors.

Electronic supplementary material The online version of this article (<https://doi.org/10.1007/s12035-018-0986-z>) contains supplementary material, which is available to authorized users.

✉ A. B. Pant
abpant@iitr.res.in; abpant@rediffmail.com

¹ System Toxicology and Health Risk Assessment Group, CSIR-Indian Institute of Toxicology Research (CSIR-IITR), MG Marg, Lucknow, Uttar Pradesh 226001, India

² Academy of Scientific & Innovative Research, CSIR-IITR Campus, Lucknow, India

apoptosis, and generation of oxidative stress [8]. Consequently, it becomes imperative to look for chemicals/compounds that can ameliorate the neuronal damages inflicted by pesticides like MCP. Phytochemicals with an inherent antioxidant property can undo or considerably minimize the damage hence caused. RV with a wider spectrum of pharmacological action is a promising neuroprotectant [9]. The presence of RV in grapes, peanuts, and red wine is well reported [10]. RV is a naturally occurring polyphenol that can easily cross the blood-brain barrier (BBB) and plays a critical role in the prevention of Alzheimer's disease (AD), Parkinson's disease (PD), Huntington's disease, and cerebral ischemia [11]. Its neuroprotective nature is attributed to its chemical structure that imparts antioxidation phenomenon enabling it to scavenge upon reactive oxygen species (ROS) [12]. In vivo and in vitro studies have demonstrated that RV inhibits A β fibril formation through sirtuin-dependent pathway [13]. Evidences from various studies have shown RV to be a neuroprotectant by scavenging hydroxyl and superoxide radicals and promoting mitochondrial biogenesis through various modulators [14]. Additionally, RV has been found effective in reducing inflammation via attenuation of sirtuin-dependent arrest of nuclear factor kappa light chain in microglia [15].

Mesenchymal stem cells (MSCs) can be used to study the neurotoxicity of MCP and neuroprotection by RV. MSCs have the inherent potential of self-renewal and differentiation into multiple lineages [16]. It has already been reported earlier by our research group that neurons derived from human umbilical cord blood stem cells serve as a robust in vitro tool for predicting the developmental neurotoxicity of MCP [17]. A number of signaling cascades operate to mitigate these neurotoxic effects and promote cell survival. One of the key components of neuronal survival is the phosphatidylinositol 3-kinase (PI3K)/Akt pathway [18]. Mitogen-activated protein kinase (MAPK) signaling pathway participates in cell survival mechanism by carrying out the posttranslational modification as well as altering the cell death machinery resulting in enhanced transcription of pro-survival genes [19]. Cell proliferation is also regulated by the MAPK cascade that activates extracellular signal-regulated kinases 1 and 2 (ERK1 and ERK2). However, the role of this cascade is also implicated in the regulation of synaptic plasticity in the adult brain. ERK signaling plays a key role in neuronal transcriptional events [20]. RV prevents Cd-induced neurotoxicity and neuronal cell death via inactivation of Erk1/2 and JNK pathways and protein phosphatase (PP2A and PP5) [21]. RV was also observed to mitigate cell death induced by oxygen and glucose deprivation (OGD) via activation of PI3K/Akt pathways [22]. It would be interesting to decipher if RV can exert its neuroprotective effects over MCP-induced neurotoxicity in MSCs and unravel the signaling cascade it follows for the same.

Materials and Methods

Reagents and Consumable

All the specified chemicals, viz., resveratrol and monocrotophos were procured from Sigma-Aldrich, India. Resveratrol (Cat No. R5010, Sigma) was dissolved in culture-grade dimethyl sulfoxide (DMSO) (Cat No. D2650, Sigma-Aldrich, India) and stored at -20°C . Monocrotophos (Cat No. 36173, St. Louis, MO, USA) was dissolved in distilled water and stored at 4°C . Alpha minimal essential medium (α -MEM) (Cat No. 12561056), MSC-qualified FBS (Cat No. 12662-029), antibiotic solution (100 \times) (Cat No. 15240062), GlutaMAXTM-I (100 \times) (Cat No. 35050-061), sodium bicarbonate (7.5%) (Cat No. 25080-094), fluorescent antibodies, and Dulbecco's phosphate-buffered saline (DPBS) (Cat No. 14200-75) were purchased from Gibco, Invitrogen, Grand Island, NY, USA. Antibodies were purchased from Millipore, USA.

Ethical Clearance for Collection and Transportation of Human Tissues

The entire study was carried out following the protocols and procedures approved by the Institutional Human Ethics Committees of CSIR-Indian Institute of Toxicology Research (CSIR-IITR) and CSM Medical University, Lucknow, India. The informed consent of parents was obtained before collecting blood from umbilical cord. Mothers enrolled in the study were of age ranging from 24.5 to 30 years. They fulfilled the entire inclusion criteria and were free from malignancy or any other systemic disorder. All experiments were performed according to institutional guidelines and regulations.

Isolation of Mesenchymal Stem Cells from Human Umbilical Cord Blood

A total of 40 blood samples (approximately 45 mL/cord) were collected from the cord vein in sterile containers having anticoagulant citrate dextrose (ACD) buffer and immediately transported to CSIR-IITR, Lucknow, for further processing. Blood was diluted 1:1 with DPBS without Ca^{2+} and Mg^{2+} , pH 7.5 (Stem Cell Technologies). MSCs were isolated as per our previous protocol [23]. Freshly isolated MSCs were cultured in plastic 25-cm² ultralow attachment culture flask (Nunc Inc.) at a density of 1×10^5 cells/mL in 5 mL α -MEM (Gibco, Life Technology, USA) supplemented with glutamax, antibiotic-antimycotic and sodium bicarbonate, and 20% MSC qualified FBS (Gibco, Life Technology, USA). Cells were allowed to adhere and maintained in humidified atmosphere at 37°C and 5% CO_2 . Half of the medium was changed every alternate day. At each passage, cells were checked for cell surface markers to

ascertain the purity of mesenchymal stem cells as described in our previous study [23]. Cells were subcultured at the confluence of 85–90% in α -MEM containing serum and essential supplement as mentioned earlier.

Cytotoxicity of MCP and RV and Non-Cytotoxic Exposure to MSCs

For determining cell viability, 3-(4,5-dimethylthiazol-2-yl)-2,5-diphenyltetrazolium bromide (MTT) assay was used [17]. MSCs were co-exposed with different concentrations of MCP (10, 100, 1000 μ M) and RV (0, 5, 10, 20 μ M) for 24 h. After completion of exposure period, 10 μ L MTT (5 mg/mL) was added in each well at a final concentration of 50 μ g/mL and the mixture was further incubated for 1 h at 37 °C. Liquid content of each well was then replaced with 100 μ L of DMSO. After 10 min, the absorbance was recorded at 550 nm using a multi-well microplate reader (Synergy HT, Bio-Tek, USA). The relative cell viability was expressed as a percentage of the untreated control group. On selection of non-cytotoxic dose of RV and MCP, proliferating human umbilical cord blood-derived mesenchymal stem cells (hUCB-MSCs) were exposed to RV (10 μ M) and MCP (100 μ M) alone, as well as in combination for 24 h.

Lipid Peroxidation Assay

Following the exposure of MCP and/or RV for 24 h, hUCB-MSCs were harvested by centrifugation at 1000 rpm for 10 min and processed for the estimation of lipid peroxidation using a commercially available kit (Lipid Peroxidation Assay Kit, Cat No. 705003, Cayman Chemicals, USA) as per the manufacturer's protocol. Cells exposed to H₂O₂ (100 μ M) for 2 h under identical conditions served as the positive control.

Glutathione Disulfide/Reduced Glutathione Ratio

The ratio of glutathione disulfide (GSSG) with respect to reduced glutathione (GSH) was assessed under the same experimental setup as that of lipid peroxidation assay (LPO) using a commercially available kit (ApoGSH Glutathione Colorimetric Assay Kit, Cat No. K261-100, Biovision, USA). The data are represented as the ratio between GSSG and GSH. Cells exposed to H₂O₂ (100 μ M) for 2 h under identical conditions were used as the positive control.

Reactive Oxygen Species Generation

MCP-induced ROS generation and RV-induced protection over MCP-damaged hUCB-MSCs were assessed using the fluorescent dye 2',7'-dichlorodihydrofluorescein diacetate (DCFH-DA, Sigma-Aldrich, USA). Briefly, cells (5×10^4

per well) were seeded in tissue culture chamber slide and allowed to adhere. Adhered cells were then exposed to various concentrations of MCP (10^{-5} to 10^{-7} M) for 24 h. Following exposure, cells were washed twice with DPBS and incubated for 30 min in the dark in serum-free culture medium containing DCFHDA (20 μ M). Slides were washed twice with DPBS and mounted for microscopic analysis. Intracellular fluorescence was measured using an upright fluorescence microscope (Nikon Eclipse 80i equipped with Nikon DS-Ri1 12.7-megapixel camera). Quantification of fluorescence was done using the image analysis software Leica Qwin 500, and data were expressed as the fold change of unexposed control. Cells exposed to H₂O₂ (100 μ M) for 2 h under identical conditions were used as a positive control.

Flow Cytometry Analysis

After exposure with MCP and/or RV, hUCB-MSCs were harvested by trypsinization and washed once with DPBS (pH 7.4). After centrifugation, the cells were stained with annexin-V and propidium iodide (PI) using the annexin V-FITC apoptosis detection kit (BD Biosciences, San Jose, CA, USA) for analysis of the translocation of phosphatidylserine from the inner to the outer leaflets of the plasma membrane. For annexin V and PI double staining, the procedure was performed according to the instructions of the manufacturer. Staurosporine (100 nM) was used as positive control. For analysis of ROS generation, cell pellets were re-suspended in 1-mL cell culture medium and incubated with 10 μ M DCFDA dye and incubated for 30 min at 37 °C, after centrifugation cells were washed with DPBS. H₂O₂ (200 μ M) was used as positive control. Analysis of mitochondrial membrane potential (MMP) was performed by using mitochondrial stain kit (Cat No. CS0390, BD Bioscience, USA). In this study, cell pellets were re-suspended in 1-mL cell culture medium containing JC-1 (10 μ M) and incubated at 37 °C for 15 min. After centrifugation, the cells were re-suspended in DPBS. Valinomycin (10 μ M) was used as positive control. The entire analysis was performed using a flow cytometer (Model: FACS BD Influx; BD Biosciences, USA).

Ultrastructural Analysis by Transmission Electron Microscopy

Cells were harvested using trypsin-EDTA and fixed in 2% glutaraldehyde for 4 h and then centrifuged. Cells in untreated control and treated groups were washed with $1 \times$ PBS (pH 7.2) and fixed in 2.5% glutaraldehyde prepared in sodium cacodylate buffer (Ladd Research Industries, USA) (pH 7.2) for 2 h at 4 °C. Cells were washed three times with 0.1 M sodium cacodylate buffer and post fixed in 1% osmium tetroxide for 2 h. Fixed cells were washed with sodium cacodylate, dehydrated in acetone series (15–100%),

and embedded in araldite-DDSA mixture (Ladd Research Industries, USA). After baking at 60 °C, blocks were cut (60–80 nm thick) by an ultramicrotome (Leica EM UC7), and sections were stained by uranyl acetate and lead citrate. Sections were then analyzed under FEI Tecnai G2 spirit twin transmission electron microscope equipped with Gatan digital CCD camera (SEM Quanta FEG, FEI Netherlands) at 80 kV.

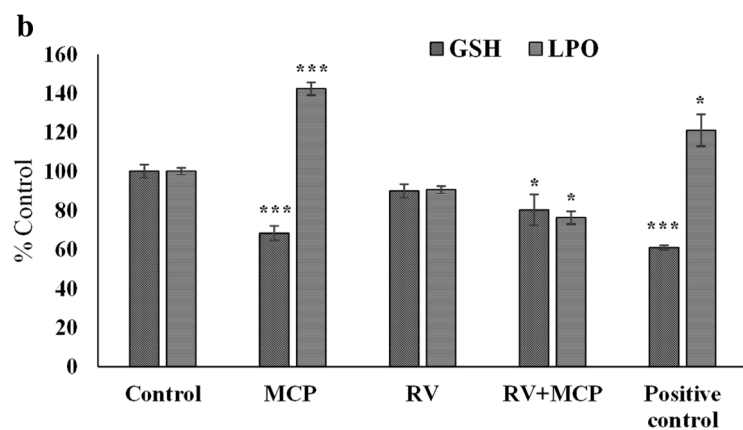
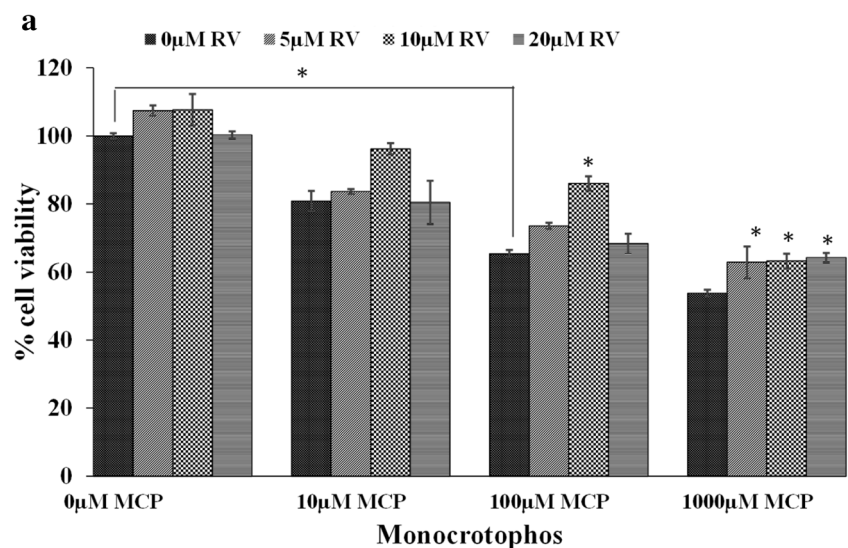
Translational Study

Western blot analysis was carried out for selected neuronal markers (nestin, β -III tubulin) and apoptosis marker proteins (cytochrome c, Bax, Bcl2, and activated caspase-3). Briefly, following MCP and/or RV exposure, cells were centrifuged and lysed using CellLytic M Cell Lysis Reagent (Cat No. C2978, Sigma, USA) supplemented with 1 \times protein inhibitor cocktail (Cat No. P8340, Sigma, USA). Protein estimation was done by Coomassie Plus™ Protein Assay (Cat No. 23236, Thermo Scientific, USA). Equal amount (50 μ g per well) of protein was loaded in 10% tricine-SDS gel and blotted on polyvinylidene fluoride (PVDF) membranes using wet transfer

system. After blocking for 1 h at 37 °C, the membranes were incubated overnight at 4 °C with primary antibodies specific for nestin and β -III tubulin (1:1000, Millipore, USA) and Bax, Bcl2, cytochrome c (cyt-c), and β -actin (1:1000, Millipore, USA).

Following western blot analysis, immune-cytochemical studies were also conducted to further decipher the expression profile of the above mentioned markers. After the completion of treatment, cells were fixed with 4% paraformaldehyde (PFA) (pH 7.4) for 30 min and then blocked for 1 h in a solution comprising of bovine serum albumin (BSA) and Triton X-100 in DPBS. Following overnight incubation with primary antibodies, cells were washed three times with DPBS to remove the unbound antibodies. Then, fluorescein isothiocyanate (FITC)-conjugated rabbit anti-mouse (1:500) and rhodamine-conjugated mouse anti-rabbit (1:500) antibodies were added to each well and kept on a rocker shaker in dark for 2 h at room temperature. Cells were then washed with DPBS three times for 5 min each. Thereafter, the cells were visualized under an upright fluorescence microscope (Nikon Eclipse 80i equipped with Nikon DS-Ri1 12.7-megapixel camera, Japan) using specific filters for FITC and rhodamine.

Fig. 1 **a** Protective efficacy of 0–20 μ M RV against 0–1000 μ M MCP in terms of percent cell viability: MTT assay performed in MSCs following the exposure to MCP and/or RV for 24 h. The values are the mean \pm SEM of three experiments each carried out in triplicate. The data are expressed as the mean of the unexposed control \pm SEM, $n = 8$, $*p < 0.05$. **b** Lipid peroxidation (LPO) and ratio of glutathione disulfide (oxidized form of glutathione) to reduced glutathione (GSSG/GSH) in hUCB-MSCs following the exposure of MCP for 24 h. Exposure of 100 μ M H₂O₂ for 2 h was used as the positive control. ($*p \leq 0.05$; $**p \leq 0.001$; $***p \leq 0.0001$)



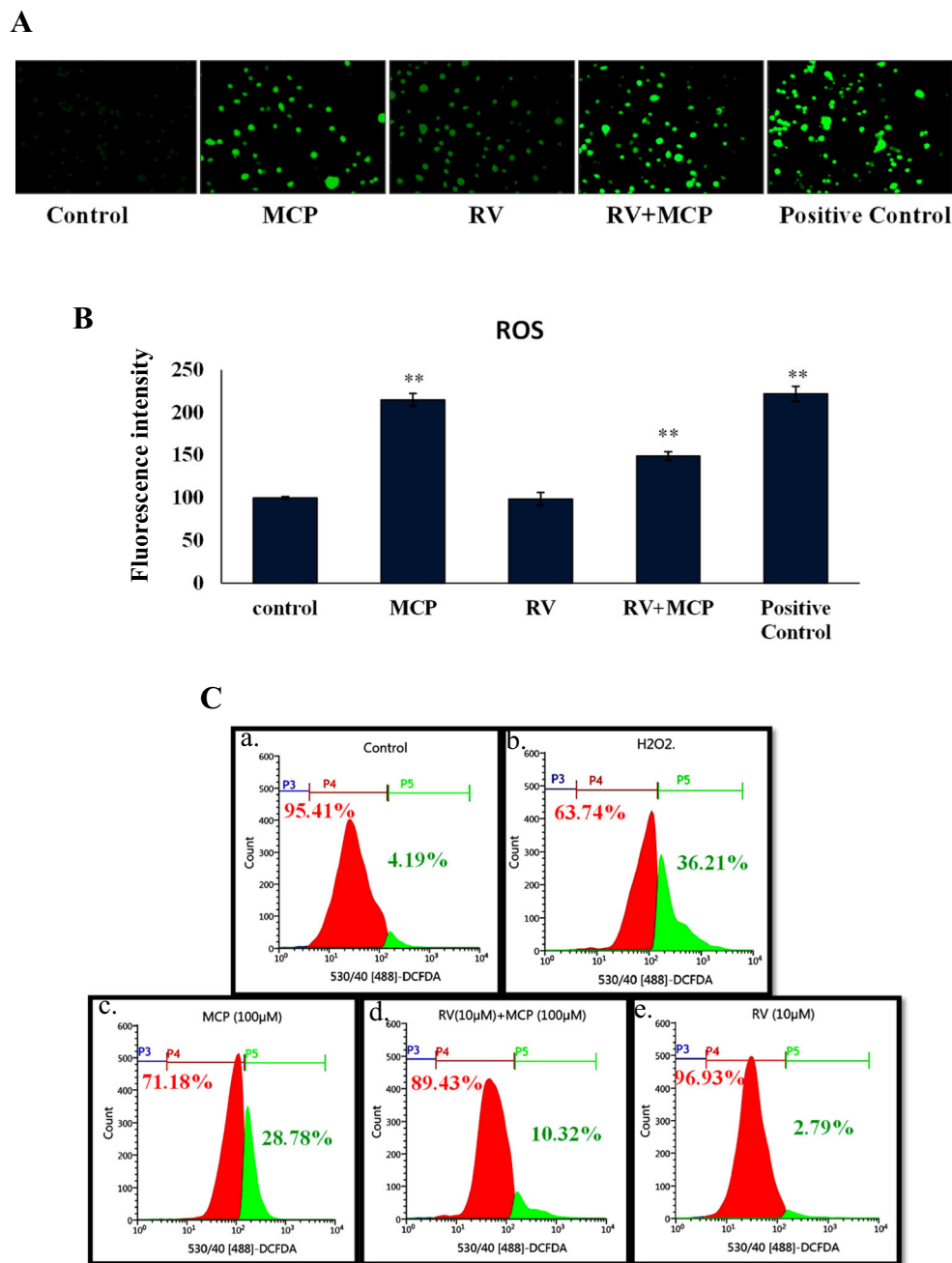
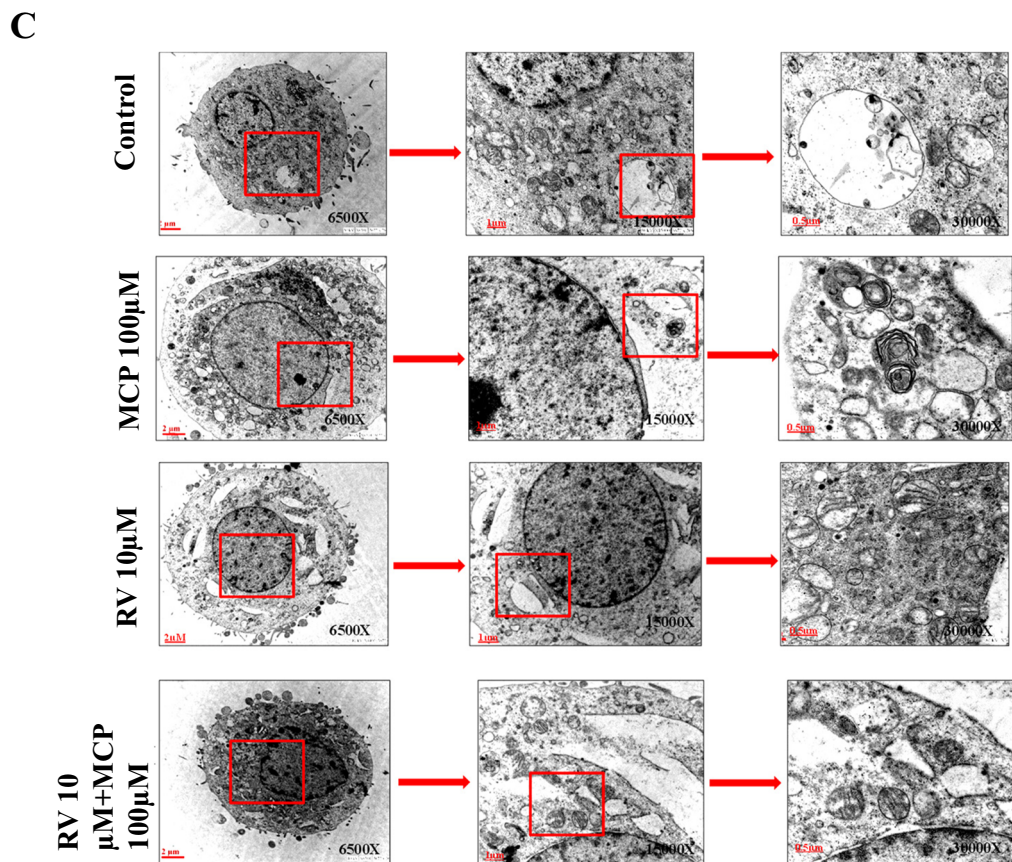
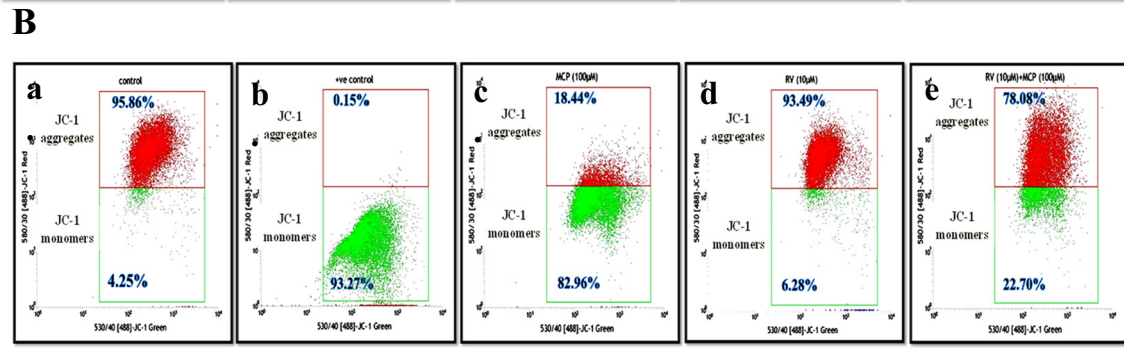
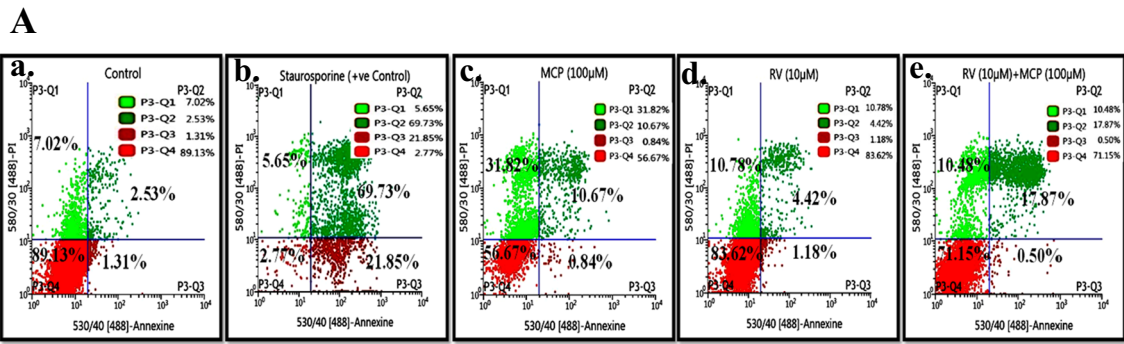


Fig. 2 RV inhibits ROS formation in MSCs exposed to MCP. **a** hUCB-MSCs were treated with 10 µM RV and/or 100 µM MCP for 24 h and incubated with 10 µM H₂-DCF-DA fluorescent dye for 20 min for the detection of total cellular ROS. Cellular and mitochondrial ROS generation was observed, and images were taken using Nikon phase-contrast cum fluorescence microscope (model 80i) attached with a 12.7-mega-pixel Nikon DS-Ri1 digital CCD cool camera. **b** Percent changes in ROS generation in hUCB-MSCs after 24-h exposure to 10 µM RV and/or 100 µM MCP were assessed by spectrofluorometric analysis.

Fluorescence intensity was measured using a multi-well microplate reader (Synergy HT; Bio-Tek) using an excitation wavelength of 485 nm and emission wavelength of 528 nm. The data are expressed as the mean of the percent of unexposed control \pm SEM, $n = 8$. * $p < 0.05$; ** $p < 0.01$; *** $p < 0.001$. **c** Flow cytometric analysis of H₂O₂ stimulated, untreated, and MCP exposed cells, with or without RV, were incubated with 10 µM DCFH-DA for 30 min and analyzed using a flow cytometer (BD Influx; BD Biosciences, USA). The red to green shift in the histogram signifies cell death due to increased ROS production

For each marker, 20 randomly selected microscopic fields were captured and analyzed for fluorescence intensity with the help of Leica Qwin 500 Image Analysis Software (Leica, Germany). The values were expressed in mean \pm SE of

percent area for fluorescence intensity covered. The values of undifferentiated cells at day 0 were used as control to calculate the differentiation-induced alterations in the expression of each neuronal marker.



Statistical Analysis

Results are expressed as the mean ± SE of the values obtained from at least three independent experiments,

carried out in triplicate. Statistical analyses were performed using one-way analysis of variance (ANOVA), namely Tukey compare to all and post hoc Dunnett’s two-sided test to compare the findings in different

Fig. 3 Resveratrol (RV) abrogates MCP-mediated apoptosis in hUCB-MSCs. **a** hUCB-MSCs were treated with RV (10 μ M) and/or MCP (100 μ M) for 24 h and then stained with Annexin-V and PI and then analyzed using a flow cytometer (BD-Influx; BD Biosciences, USA). The cells in the quadrant P3-Q1 denote necrotic cells; P3-Q2 denotes late apoptotic cells; P3-Q3 denotes early apoptotic cells; P3-Q4 denotes healthy viable cells. **b** hUCB-MSCs were treated with RV (10 μ M) and/or MCP (100 μ M) for 24 h, stained with JC-1, and then analyzed using a flow cytometer (BD Influx; BD Biosciences, USA). The JC1 aggregates are present in viable cells, while these aggregates dissociated into JC1 monomers in cells undergoing cell death. Analysis was done by BDFACS™ software v.1.0. **c** hUCB-MSCs were treated with RV (10 μ M) and/or MCP (100 μ M) for 24 h. Mitochondrial morphological changes were analyzed using transmission electron microscopy using different magnification for comparative higher resolution as described under “Materials and Methods” section. Scale bar, 2 μ m \times 6500, 1 μ m \times 15,000, and 0.5 μ m and \times 30,000

groups with the untreated control group. The values, $p < 0.05$, were considered significant.

Results

Resveratrol Protects hUCB-MSCs Against MCP-Induced Cytotoxicity

Cell viability was measured in the presence of different concentrations of MCP; the 10 μ M concentration of MCP showed toxicity even in the presence of different concentrations of RV with no statistical significance. But the exposure of 100 μ M of MCP shows significant toxicity against different concentrations of RV. Cell viability got decreased up to 65–80% in a concentration-dependent manner (Fig. 1a). RV alone enhanced cell viability at different concentrations. Cells subjected to the co-exposure of MCP and RV show reduced cell death. However, RV failed to protect the cells against MCP at higher concentrations like 1000 μ M. Although RV at 20 μ M concentration inhibited cell death in hUCB-MSCs, induced by varying concentrations of MCP (1–1000 μ M), at 10 μ M, it effectively prevented cell death induced by 100 μ M MCP (Fig. 1a) We therefore selected 100 μ M MCP and 10 μ M RV to further investigate the mechanism followed by RV that is responsible for its neuroprotective effect.

Antioxidant Properties of RV

MCP-induced alteration and RV-mediated protection can be seen in Fig. 1b. hUCB-MSCs exposed to MCP show increased LPO ($142 \pm 3.1\%$) in comparison to unexposed cells ($100 \pm 1.73\%$), while in co-exposed cells, percentage of LPO was found to be even lesser ($76.3 \pm 3.2\%$) (Fig. 1b). This shows the protective property of RV wherein it restores the damaged lipid membrane found in toxicant exposed cells. Ratio between GSSG and GSH in MCP and RV exposed cells alone as well as in combination is summarized in Fig. 1b.

hUCB-MSCs exposed with MCP have decreased GSH production ($68 \pm 3.7\%$) as compared with unexposed cells ($100 \pm 3.4\%$), while in the case of co-exposure of RV with MCP, cells show increased percent of GSH production ($113.6 \pm 5.2\%$) (Fig. 1b). This result indicates a protective role of RV against MCP-induced cell damage via reduced GSH production.

To further authenticate this, we conducted experiments to see whether RV could affect MCP-induced intracellular ROS accumulation in hUCB-MSCs. Microscopic study shows that ROS generation in MCP-insulted cells was around 200% in comparison to control (100%) while RV-induced protection when co-exposed with MCP and reduced ROS levels up to 150% (Fig. 2a, b). Likewise, flow cytometry analysis divulged the pattern of ROS generation in hUCB-MSC cells exposed with MCP and/or RV (Fig. 2c). Flow cytometry analysis was done in such manner that three continuous horizontal population gates (P3, P4, and P5) were placed in histogram showing emission at 530 ± 40 nm. The emission order in these gates was $P3 < P4 < P5$. Therefore, P3 gate contains unstained population (in blue), P4 contains stained, live, and healthy cells with normal ROS levels (in red), and P5 contains damaged and unhealthy cells with high level of ROS generation (in green). Hence, the higher the ROS generation, the higher will be the emission at 530 ± 40 nm, which leads to the shifting of peak towards right, i.e., from P3, P4, to P5 gate. In Fig. 2c, minimum emission at 530 ± 40 nm was seen in the case of unstained untreated cells. The control set (untreated but stained) had the basal level of ROS, and emission at 530 ± 40 nm was recorded (Fig. 2C (a)) which showed that 95.41% cells were healthy (red) and only 4.19% cells exhibited high ROS level (green). While in positive control, the H₂O₂ (100 μ M) treated cells (Fig. 2C (b)) showed extensive oxidative damage where 36.21% cells were affected. MCP (100 μ M) treated cells around 28.78% of ROS generation was seen (Fig. 2C (c)) in comparison to the control one. When cells were co-exposed with RV (10 μ M) and MCP (100 μ M), a significant restoration of oxidative damage was seen (Fig. 2C (d)). Even when cells were treated with RV (10 μ M) alone, there was minimum ROS production and conditions were very much similar to the control set (Fig. 2C (e)). As per the above inferences, the neuroprotective potential of RV over MCP exposure is postulated.

Levels of Annexin-V-FITC and PI

We investigated the changes in plasma membrane asymmetry (using the annexin-V and PI double-staining method) to quantify the population of dead cells. With this method, cells stained singly positive for PI are considered mostly necrotic cells and cells stained singly positive for annexin-V are considered mostly in early phase of apoptosis, but cells that are stained double positive are either necrotic or apoptotic. The unexposed control group recorded least percentage of necrotic

and apoptotic cells (Fig. 3A (a)), whereas the cells exposed to staurosporine have shown cell damage and only 2.77% of cells are found to be live (Fig. 3A (b)). We found that exposure of hUCB-MSCs to 100 μ M MCP alone for 24 h also increased the number of damaged cells in comparison to control (56.67 vs 89.13%) (Fig. 3A (c)). On the other hand, cells treated with RV are comparable to that of control cells (Fig. 3A (d)). However, co-treatment of these cells with MCP and RV markedly reduced the population of dead cells, and more live cells were seen (71.15%) (Fig. 3A (e)). This observation was consistent with the cell viability data as shown in Fig. 1a, thus confirming that RV itself is not cytotoxic rather it abrogated the damaging effect of MCP.

MCP and/or RV Induced Alteration in MMP

To investigate whether MCP leads to change in MMP in hUCB-MSCs, we further administered JC-1 dye in MCP-insulted cells. JC-1 gets excited at \approx 490 nm and emits wavelength at \approx 530 \pm 40 nm (for JC-1 monomers—green) and at \approx 580 \pm 30 nm (for JC-1 aggregates—red). The higher the ratio

of monomer to the aggregates (530 \pm 40:580 \pm 30), the higher will be the membrane depolarization. When the membrane potential of mitochondria is high, JC-1 moves inside mitochondria and gets polymerized into its aggregates, while during low MMP, monomers of JC-1 are formed. When mitochondria are in a good condition, their membrane potential is high and the entrance of JC-1 is fast, but toxicants can affect this membrane potential resulting in mitochondrial damage, which leads to an overall reduction in membrane potential. In Fig. 3B (a), the cells in control group were 95.86% healthy and lay under JC-1 aggregate region (red). Only 4.25% of cells had JC-1 monomers due to loss in MMP. We used valinomycin (1 μ g/mL), a known MMP disrupter, as the positive control, and its effect can be clearly seen in Fig. 3B (b), with increased number of cells in JC-1 monomer region (93.27%) and lesser number of viable cells (\approx 0%). In Fig. 3B (c), an enhancement in the number of JC-1 monomeric cells was observed (i.e., up to 82.96%), due to induced MMP loss by MCP (100 μ M) treatment, while 18.44% cells showed the presence of JC-1 aggregates, hence were viable. The MMP-enhancing role of RV can be observed in Fig. 3B

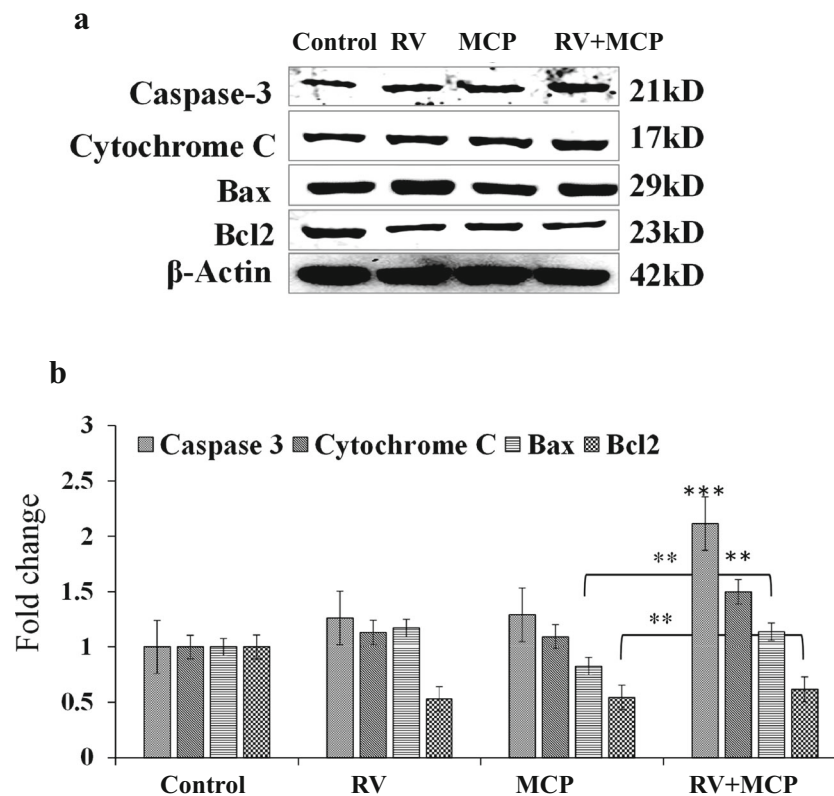


Fig. 4 Alterations in the expression of proteins, involved in the induction of apoptosis, were studied in hUCB-MSCs exposed to MCP (100 μ M) and/or RV (10 μ M) for 24 h. Beta-actin was used as the internal control to normalize the data. Untreated control; cells exposed to MCP for 24 h; cells exposed with RV; and cells exposed to MCP and/or RV for 24 h; molecular weight of protein studied: activated caspase-3 (21 kDa), cytochrome-c (17 kDa), Bax (29 kDa), Bcl2 (23 kDa), and β -actin

(42 kDa). Fold changes: The relative protein level was calculated according to the densitometry of each band, normalized according to the internal control. The control group was arbitrarily set at 1.0 for ease of comparison for normalization. Quantification was done in Gel Documentation System (Alpha Innotech, USA) with the help of AlphaEase FC StandAlone V.4.0 software

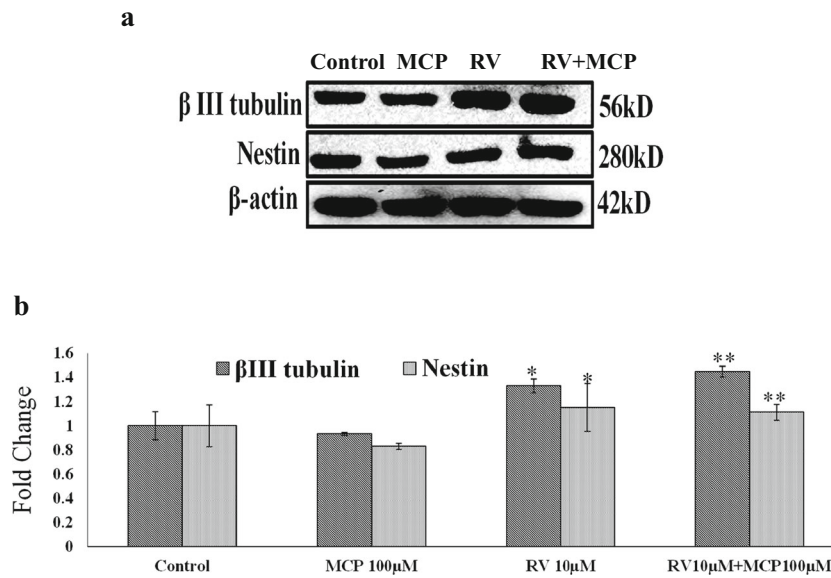
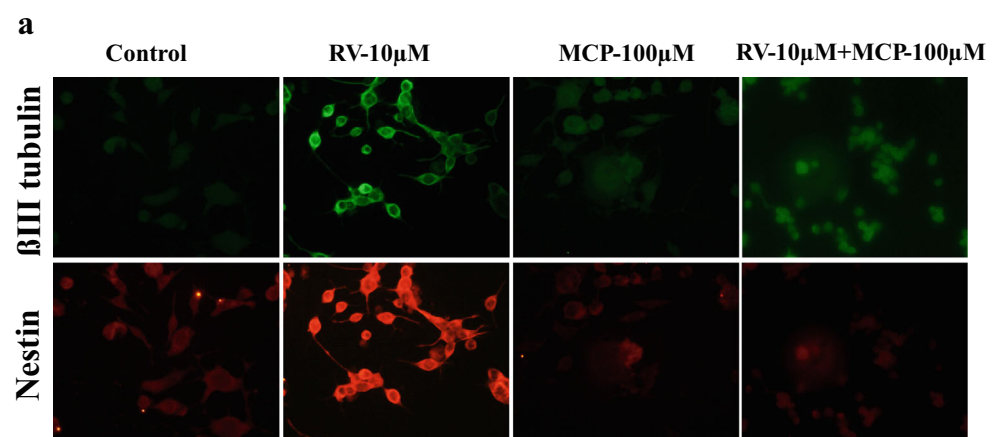


Fig. 5 Alterations in the expression of early neuronal markers were studied in hUCB-MSCs exposed to MCP (100 μ M) and/or RV (10 μ M) for 24 h. β -Actin was used as the internal control to normalize the data. Untreated control; cells exposed to MCP for 24 h; cells exposed with RV; and cells exposed to MCP and/or RV for 24 h; molecular weight of protein studied: beta III-tubulin (56 kDa) and nestin (280 kDa) and β -

actin (42 kDa). The relative protein level was calculated according to the densitometry reading of each band, which was then normalized according to the internal control. The control group was arbitrarily set at 1.0 for ease of comparison for normalization. Quantification was done in Gel Documentation System (Alpha Innotech, USA) with the help of AlphaEase FC StandAlone V.4.0 software

Fig. 6 Immunocytochemical study was carried out to detect changes in neuronal markers, viz., β -III tubulin and nestin under MCP, RV, and/or MCP-exposed hUCB-MSCs. Percent intensities were detected by ImageJ 1.48v, Nikon, NIS, USA. Fold changes shown in **b**



(d) wherein cells were treated with RV (10 μ M) alone. The toxic effect of MCP (100 μ M) was significantly restored by up to 78.08% when cells were co-exposed to RV (10 μ M) and MCP (100 μ M) (Fig. 3B (e)).

Mitochondrial Anomalies Analyzed by TEM

We investigated the effect of RV on MCP-induced changes in the topography of mitochondria. To determine the changes in mitochondrial morphology, we applied transmission electron microscopy analysis. Following the exposure to 100 μ M MCP, majority of mitochondria in the hUCB-MSCs were swollen and few of them lost cristae (Fig. 3c—MCP 100 μ M). However, RV and MCP-exposed cells mostly abrogated these morphological changes (Fig. 3c—RV + MCP).

Changes in Protein Expressions

In western blot analysis, a significant increase in protein expression of apoptosis markers like cytochrome c (17 kD), Bax (29 kD), Bcl2 (23 kD), and caspase-3 (21 kD) was observed in cells exposed to MCP (100 μ M) for 24 h. The cells also showed a significant increase in the expression of cytochrome c, Bax, and activated caspase-3 when co-exposed to RV and MCP for 24 h; however, the elevated levels of Bax, activated caspase-3, and cytochrome c were restored in comparison to the MCP-exposed cells (Fig. 4). In the case of Bcl2, MCP-exposed cells have showed a significant decrease in expression, that is, 0.50-fold in comparison with the control, and in the co-treatment group, RV + MCP-exposed cells showed 0.69-fold expression of BCL2 in comparison with the control.

Influence of RV on Neuronal Markers in the Cells Exposed to MCP

It is reported that MSCs express early neuronal markers in the undifferentiated state [24]. Our group also reported the efficacy of hUCB-MSCs into neuronal subtypes in the presence of NGF-50 ng/mL and RV-10 μ M [25]. Here, we investigated the effect of MCP on neuronal markers by immunocytochemical analysis as well as western blotting. When cells were lysed and subjected to western blotting (Fig. 5a), it shows significant restoration of neuronal marker expression status in RV and/or RV-exposed cells in contrast to MCP-exposed cells in which these markers are prominently down-regulated. Data in Fig. 5b shows that MCP-exposed cells have statistically significant diminished expression of neuronal markers, while cells co-exposed to RV and MCP show restoration of early stage neuronal markers, viz., nestin and β -III tubulin in comparison to MCP (Fig. 6).

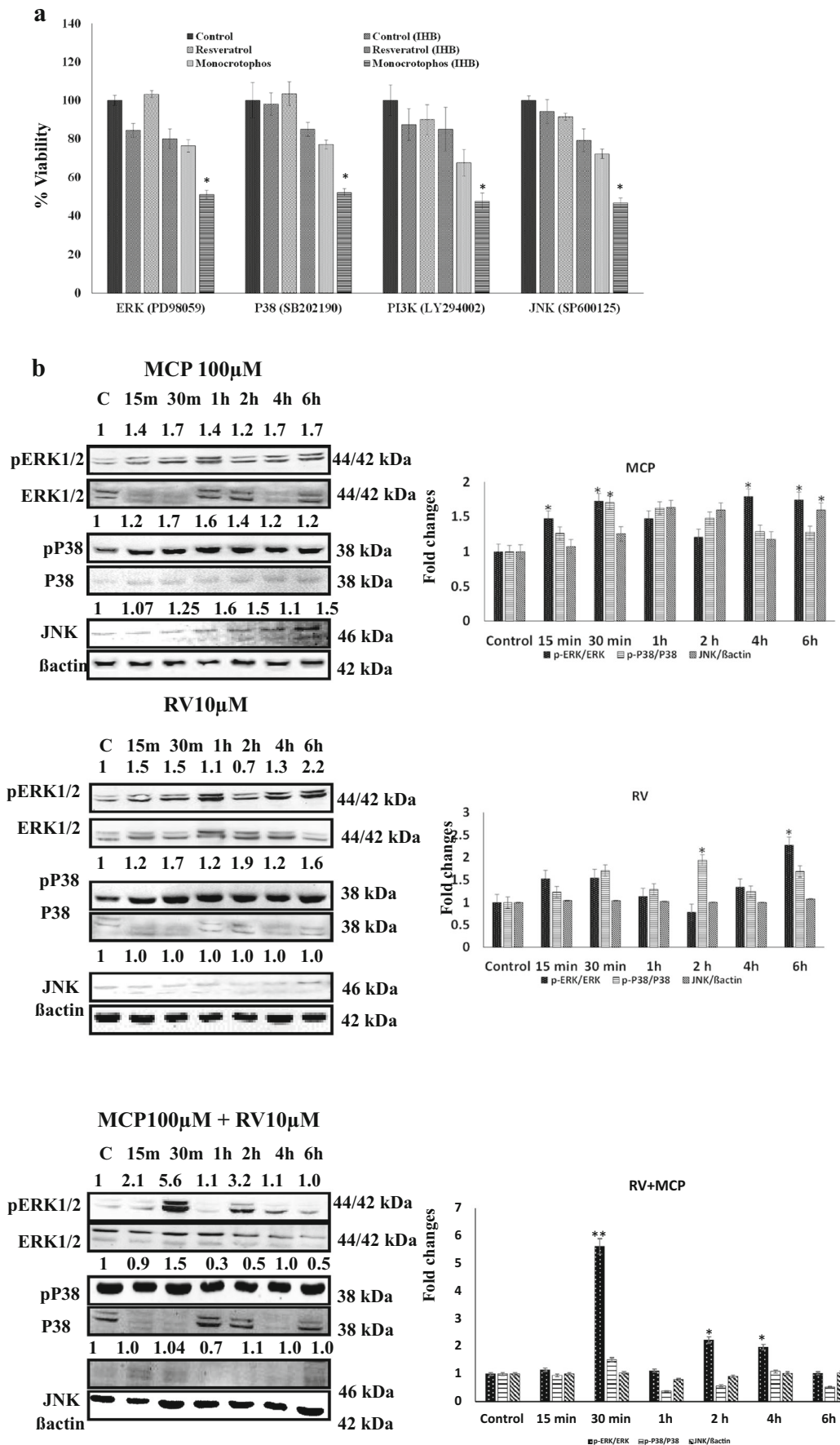
RV Triggers the MAPK and PI3K Signaling Pathways in hUCB-MSCs Exposed to MCP

We examined the role of MAPK and PI3K signaling molecules in restoration of MCP-induced cytotoxicity in hUCB-MSCs. As shown in Fig. 7, after 24-h exposure to MCP alone, JNK1/2, ERK, and p38 were significantly activated (phosphorylated). However, when the cells were co-exposed to RV and MCP, these changes were abrogated. We further have chosen selective inhibitors of these signaling proteins to probe their functional roles. The hUCB-MSCs were first pre-exposed to each of the inhibitors and then cultured in the presence of MCP with or without RV. As shown in Fig. 7a (MTT assay) and Fig. 7b (western blot study), SP600125 (an inhibitor of JNK1, JNK2, and JNK3), SB202190 (an inhibitor of p38 MAPK- β), and U0126 [an inhibitor of MEK1/2 (MAPK or ERK kinase)] each significantly reduced MCP-induced cell death in a concentration-dependent manner. On the contrary, RV's protective effect was strongly diminished by LY294002 (a PI3K inhibitor) depicted in Fig. 7c, d. Taken together, these results suggest that, however, the MAPK signaling pathways (JNK, p38, and ERK) are involved in MCP-induced oxidative cell death and activation of the PI3K signaling pathway is specifically associated with neuroprotective effect of RV.

Discussion

Toxicological research helps us probe into cellular, molecular, tissue, organ and organ system changes, and system-wide pathologies [26]. The present study describes

Fig. 7 Activation of JNK, p38, and ERK signaling pathways after MCP and/or RV treatment. **a** Study of cell viability in the presence of inhibitors. hUCB-MSCs were treated with MCP (100 μ M) and RV (10 μ M) with inhibitors of ERK (PD98059), p38 (SB202190), JNK (SP600125), and PI3K (LY294002), respectively. hUCB-MSCs were treated with MCP (100 μ M) and/or RV (10 μ M) **(b)**. After incubation for the indicated length of time, cell extracts were subjected to SDS-PAGE and immunoblotting with antibodies specific for phospho-JNK (Thr183/Tyr185), phospho-p38 (Thr180/Tyr182), and phospho-ERK (Thr202/Tyr204). Membranes were stripped and re-probed for total JNK, total p38, or total ERK. The ratio of phosphorylated protein was calculated from three independent experiments (shown under each immunoblot of the phosphorylated protein). The relative protein level for the phosphorylated protein was calculated according to the densitometry reading of each band, which was then normalized according to the densitometry reading for the corresponding total protein level. The control group was arbitrarily set at 1.0 for ease of comparison. Involvement of PI3K in RV-induced signaling: hUCB-MSCs were treated with MCP (100 μ M) and RV (10 μ M) with inhibitors of PI3K (LY294002) in **c**. The relative protein level was calculated according to the densitometry reading of each band, which was then normalized according to the densitometry reading for the corresponding total protein level



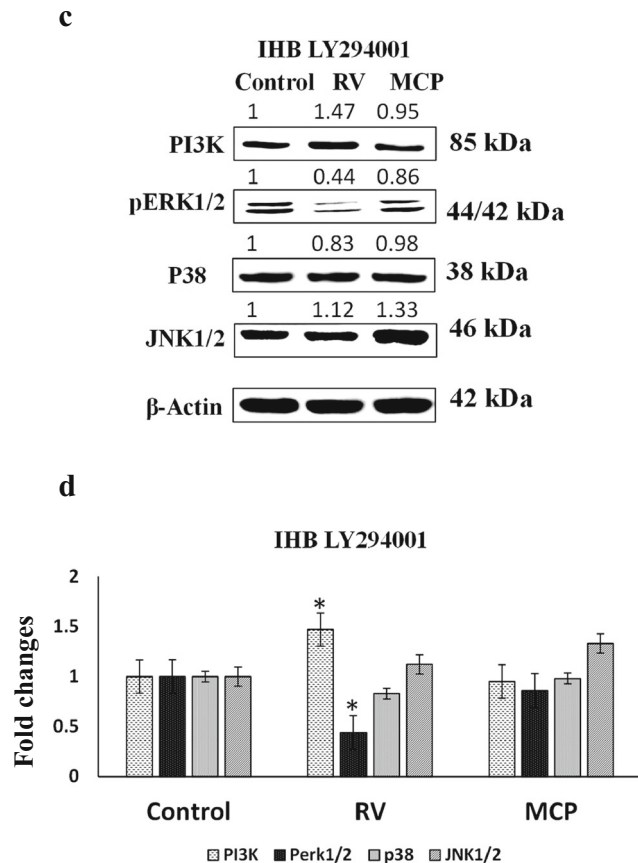


Fig. 7 (continued)

health risks that are associated with pesticide exposure [27]. It aims to find out the toxicity in hUCB-MSCs due to MCP exposure and its protection by RV along with the signaling molecules involved (Fig. 8). Brain's high lipid content makes it vulnerable towards MCP toxicity [28]. Oxidative stress induced by OP (MCP) intoxication is associated with elevated lipid peroxidation and decreased antioxidant defense. It also induces the production of reactive oxygen species by several biochemical mechanisms [29]. ROS generation subsequently results in lipid peroxidation, protein oxidation, modulation of gene expression, alteration of redox status, certain diseases, and premature aging. Reduced glutathione is the principal antioxidant molecule for scavenging and detoxification of free radicals and preventing oxidative damage [30]. Therefore, if we consider the GSH level, it is reported that increased GSSG/GSH ratio propels PC12 cells towards apoptosis [31]. In hUCB-MSCs also, GSSG/GSH ratio was found to be higher in MCP-exposed cells.

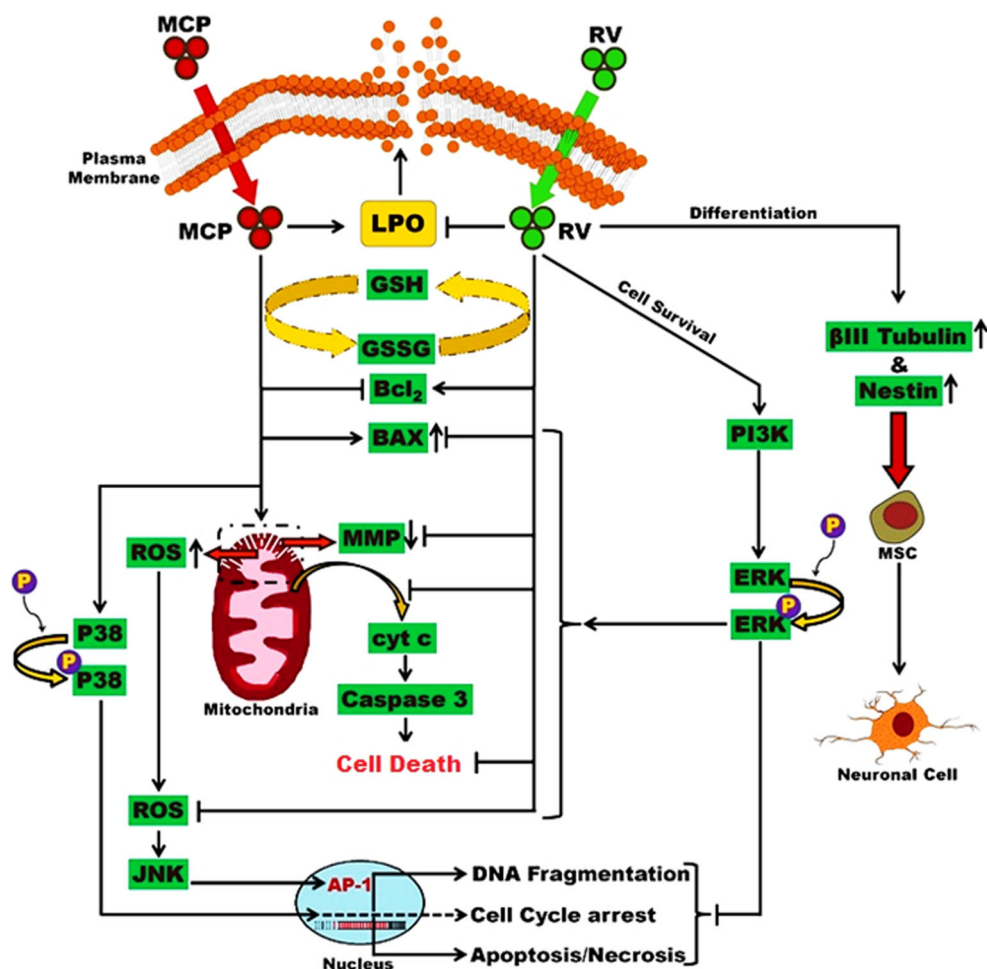
Results indicate that MCP also mediates cellular damage via apoptosis. Apoptosis manifests its effect

via two major execution programs downstream of the death signal: the caspase pathway and organelle dysfunction. Out of them, mitochondrial dysfunction is the best characterized so far. As the Bcl-2 family members reside upstream of irreversible cellular damage and focus much of their efforts at the level of mitochondria, they play a pivotal role in the selection of cell fate [32]. Bcl-2 molecules are considered as “guards of mitochondrial gate.” On the other hand, pro-apoptotic molecule like Bax gets translocated to the mitochondria. cyt-c-mediated mechanism has been suggested to occur via potential differences which are associated with mitochondrial swelling and as a consequence would result in the rupture of the outer mitochondrial membrane that leads to the release of cyt-c into the cytoplasm [33]. Thus, in some system, dissipation of MMP has been associated with cyt-c release from mitochondria [34]. MMP study showed significant perturbation in the mitochondrial potential in MCP-exposed hUCB-MSCs.

TEM study results clearly demonstrate mitochondrial damage. The inhibitory effect of MCP over neuronal differentiation has also been proved earlier wherein MCP-exposed neural stem cells of rat brain exhibited diminished expression of TrkA and other key signaling molecules as well as neural markers associated with neuronal differentiation [35]. However, the damages incurred by hUCB-MSCs after exposure to MCP were seemingly restored by RV which is primarily due to the transient, non-cytotoxic, S-phase delay induced by RV as well as its antioxidant properties [36, 37]. RV exerted its neuroprotective effects at lower concentrations of MCP but failed to do so at higher ones. This can possibly be attributed to the immense amount of stress resulting due to exposure to such high concentrations of MCP [37].

It has already been reported in earlier studies that RV possesses a direct radical scavenging property [38]. ROS generation is a trademark of MCP-induced toxicity in PC12 [39], SHSY-5Y, and stem cells [40, 41]. The neuroprotective role of RV against MCP-induced neurotoxicity has already been proved in in vitro neuronal model of PC12 cells [42]. The hUCB-MSCs also demonstrated a similar pattern of neuroprotection by RV and nerve growth factor [23, 25]. The results obtained are in lines of an earlier study which reported that RV exerted direct significant protection in cerebral cortical astrocytes against 100 μ M H₂O₂ [43]. Moreover, RV itself does not show any evidence of apoptosis, and the MCP and RV co-exposed group shows significant neuroprotection against MCP-induced neurotoxicity in these cells. MMP study also showed significant protection in co-exposed

Fig. 8 Diagrammatic representation of MCP-induced neurotoxicity and restoration of cell survival and neurogenesis by RV. RV manifests its effects via PI3K-associated pathway. RV maintains neuronal integrity along with induction of neuronal differentiation



hUCB-MSCs against MCP-induced alterations in mitochondrial potential. The change in MMP has been postulated to be an early obligate event in the apoptotic signaling pathway. In previous studies, it has been reported that MCP causes alteration in MMP in PC12 cells [8], stem cells [44], and neuroblastoma cell lines. Ultrastructural studies show restoration of mitochondria structure in MCP and RV co-exposed cells. It has also been proved earlier by our research group that mitochondrial dysfunction is an earlier demarcating event in MCP-induced oxidative toxicity [45]. Consequently, we hypothesize here that RV stimulates a direct signaling pathway which shows increased antioxidant activity in hUCB-MSCs and lowers the effect of MCP-induced toxicity.

Earlier studies showed that RV could alter the activity of MAPKs and PI3K/Akt signaling molecules [26], which are regulated by phosphorylation. To know the signaling molecules associated with mechanistic studies of RV in hUCB-MSCs, we focused on pathway

involving pERK^{1/2}, P-38, and JNK. Our results clearly indicate the involvement of PI3K in RV-mediated cell survival. Studies conducted earlier on subarachnoid hemorrhage (SAH) rats [46] and glucose-induced neurotoxicity of PC12 cells [21] have also reported PI3K-mediated pathway as one of the primary pathways operating in the case of RV-induced neuroprotection. Therefore, the present study emphasizes the neuroprotective role of RV associated with PI3K-mediated signaling cascade in MCP-induced neurotoxicity of hUCB-MSCs and its possible implementation as a therapeutic intervention in MCP or OP pesticide-induced neurodegeneration.

Funding Information Financial support from University Grants Commission, Department of Science and Technology, Ministry of Science & Technology, Government of India, New Delhi, India [Grant No. SR/SO/Z 36/2007/91/10] and Council of Scientific & Industrial Research, Government of India, New Delhi, India [Grant No. BSC0111/INDEPTH/ CSIR Network Project] is acknowledged.

Compliance with Ethical Standards

Conflict of Interest The authors declare that they have no conflict of interest.

References

- Moser VC (2011) Functional assays for neurotoxicity testing. *Toxicol Pathol* 39(1):36–45
- Cannon JR, Greenamyre JT (2011) The role of environmental exposures in neurodegeneration and neurodegenerative diseases. *Toxicol Sci*: p. kfr239
- Drachman DA (2006) Aging of the brain, entropy, and Alzheimer disease. *Neurology* 67(8):1340–1352
- Roberts RA, Aschner M, Calligaro D, Guilarte TR, Hanig JP, Herr DW, Hudzik TJ, Jeromin A et al (2015) Translational biomarkers of neurotoxicity: a Health and Environmental Sciences Institute perspective on the way forward. *Toxicol Sci* 148(2):332–340
- Moreno-Banda G, Blanco-Muñoz J, Lacasaña M, Rothenberg SJ, Aguilar-Garduño C, Gamboa R, Pérez-Méndez O (2009) Maternal exposure to floricultural work during pregnancy, PON1 Q192R polymorphisms and the risk of low birth weight. *Sci Total Environ* 407(21):5478–5485
- Pilkington A, Buchanan D, Jamal GA, Gillham R, Hansen S, Kidd M, Hurley JF, Soutar CA (2001) An epidemiological study of the relations between exposure to organophosphate pesticides and indices of chronic peripheral neuropathy and neuropsychological abnormalities in sheep farmers and dippers. *Occup Environ Med* 58(11):702–710
- Slotkin TA, Seidler FJ (2012) Developmental neurotoxicity of organophosphates targets cell cycle and apoptosis, revealed by transcriptional profiles in vivo and in vitro. *Neurotoxicol Teratol* 34(2): 232–241
- Kashyap MP, Singh AK, Kumar V, Tripathi VK, Srivastava RK, Agrawal M, Khanna VK, Yadav S et al (2011) Monocrotophos induced apoptosis in PC12 cells: role of xenobiotic metabolizing cytochrome P450s. *PLoS One* 6(3):e17757
- Pervaiz S, Holme AL (2009) Resveratrol: its biologic targets and functional activity. *Antioxid Redox Signal* 11(11):2851–2897
- Soleas GJ, Diamandis EP, Goldberg DM (1997) Resveratrol: a molecule whose time has come? And gone? *Clin Biochem* 30(2): 91–113
- Rege SD et al (2014) Neuroprotective effects of resveratrol in Alzheimer disease pathology. *Front Aging Neurosci* 6(218):1–12
- Menard C, Bastianetto S, Quirion R (2013) Neuroprotective effects of resveratrol and epigallocatechin gallate polyphenols are mediated by the activation of protein kinase C gamma. *Front Cell Neurosci* 7:281
- Bonda DJ, Lee HG, Camins A, Pallàs M, Casadesus G, Smith MA, Zhu X (2011) The sirtuin pathway in ageing and Alzheimer disease: mechanistic and therapeutic considerations. *The Lancet Neurology* 10(3):275–279
- Granzotto A, Zatta P (2011) Resveratrol acts not through anti-aggregative pathways but mainly via its scavenging properties against A β and A β -metal complexes toxicity. *PLoS One* 6(6): e21565
- Granzotto A, Zatta P (2014) Resveratrol and Alzheimer's disease: message in a bottle on red wine and cognition. *Front Aging Neurosci* 6:95
- Neirincx V, Coste C, Rogister B, Wislet-Gendebien S (2013) Concise review: adult mesenchymal stem cells, adult neural crest stem cells, and therapy of neurological pathologies: a state of play. *Stem Cells Transl Med* 2(4):284–296
- Kashyap MP, Kumar V, Singh AK, Tripathi VK, Jahan S, Pandey A, Srivastava RK, Khanna VK et al (2015) Differentiating neurons derived from human umbilical cord blood stem cells work as a test system for developmental neurotoxicity. *Mol Neurobiol* 51(2):791–807
- Uranga RM, Katz S, Salvador GA (2013) Enhanced phosphatidylinositol 3-kinase (PI3K)/Akt signaling has pleiotropic targets in hippocampal neurons exposed to iron-induced oxidative stress. *J Biol Chem* 288(27):19773–19784
- Bonni A, Brunet A, West AE, Datta SR, Takasu MA, Greenberg ME (1999) Cell survival promoted by the Ras-MAPK signaling pathway by transcription-dependent and-independent mechanisms. *Science* 286(5443):1358–1362
- Thomas GM, Huganir RL (2004) MAPK cascade signalling and synaptic plasticity. *Nat Rev Neurosci* 5(3):173–183
- Liu M-H, Yuan C, He J, Tan TP, Wu SJ, Fu HY, Liu J, Yu S et al (2015) Resveratrol protects PC12 cells from high glucose-induced neurotoxicity via PI3K/Akt/FoxO3a pathway. *Cell Mol Neurobiol* 35(4):513–522
- Singh N, Agrawal M, Doré S (2013) Neuroprotective properties and mechanisms of resveratrol in in vitro and in vivo experimental cerebral stroke models. *ACS Chem Neurosci* 4(8):1151–1162
- Jahan S et al (2017) PKA-GSK3 β and β -catenin signaling play a critical role in trans-resveratrol mediated neuronal differentiation in human cord blood stem cells. *Molecular Neurobiology*: p. 1–12
- Pallàs M, Porquet D, Vicente A, Sanfeliu C (2013) Resveratrol: new avenues for a natural compound in neuroprotection. *Curr Pharm Des* 19(38):6726–6731
- Jahan S, Kumar D, Kumar A, Rajpurohit CS, Singh S, Srivastava A, Pandey A, Pant AB (2017) Neurotrophic factor mediated neuronal differentiation of human cord blood mesenchymal stem cells and their applicability to assess the developmental neurotoxicity. *Biochem Biophys Res Commun* 482(4):961–967
- Gilden RC, Huffling K, Sattler B (2010) Pesticides and health risks. *J Obstet Gynecol Neonatal Nurs* 39(1):103–110
- Whyatt, R.M., et al., Within-and between-home variability in indoor-air insecticide levels during pregnancy among an inner-city cohort from New York City. *Environmental health perspectives*, 2007: p. 383–389
- Kazi AI, Oommen A (2012) Monocrotophos induced oxidative damage associates with severe acetylcholinesterase inhibition in rat brain. *Neurotoxicology* 33(2):156–161
- Kennedy, C.J. and K.B. Tierney, Xenobiotic protection/resistance mechanisms in organisms, in *Environmental Toxicology*. 2013, Springer. p. 689–721
- Hayes JD, McLellan LI (1999) Glutathione and glutathione-dependent enzymes represent a co-ordinately regulated defence against oxidative stress. *Free Radic Res* 31(4):273–300
- Hiroi M, Ogihara T, Hirano K, Hasegawa M, Morinobu T, Tamai H, Niki E (2005) Regulation of apoptosis by glutathione redox state in PC12 cells exposed simultaneously to iron and ascorbic acid. *Free Radic Biol Med* 38(8):1057–1072
- Dietrich A, Mueller T, Paschke R, Kalinowski B, Behlendorf T, Reipsch F, Fruehauf A, Schmoll HJ et al (2008) 2-(4-(Tetrahydro-2 H-pyran-2-yloxy)-undecyl)-propane-1, 3-diamminedichloroplatinum (II): a novel platinum compound that overcomes cisplatin resistance and induces apoptosis by mechanisms different from that of cisplatin. *J Med Chem* 51(17):5413–5422
- Kinnally KW, Antonsson B (2007) A tale of two mitochondrial channels, MAC and PTP, in apoptosis. *Apoptosis* 12(5):857–868
- Galluzzi L, Maiuri MC, Vitale I, Zischka H, Castedo M, Zitvogel L, Kroemer G (2007) Cell death modalities: classification and pathophysiological implications. *Cell Death Differ* 14(7):1237–1242
- Kumar V et al (2015) Molecular mechanism of switching of TrkA/p75NTR signaling in monocrotophos induced neurotoxicity. *Sci Rep*. 5

36. Fukui M, Choi HJ, Zhu BT (2010) Mechanism for the protective effect of resveratrol against oxidative stress-induced neuronal death. *Free Radic Biol Med* 49(5):800–813
37. Denissova NG et al (2011) Resveratrol protects mouse embryonic stem cells from ionizing radiation by accelerating recovery from DNA strand breakage. *Carcinogenesis*, p. bgr236
38. Reiter RJ et al (2007) Melatonin and its metabolites: new findings regarding their production and their radical scavenging actions. *Acta Biochimica Polonica-English Edition* 54(1):1
39. Agrawal M, Kumar V, Kashyap MP, Khanna VK, Randhawa GS, Pant AB (2011) Ischemic insult induced apoptotic changes in PC12 cells: protection by trans resveratrol. *Eur J Pharmacol* 666(1):5–11
40. Zou C, Kou R, Gao Y, Xie K, Song F (2013) Activation of mitochondria-mediated apoptotic pathway in tri-ortho-cresyl phosphate-induced delayed neuropathy. *Neurochem Int* 62(7):965–972
41. Karami-Mohajeri S, Abdollahi M (2013) Mitochondrial dysfunction and organophosphorus compounds. *Toxicol Appl Pharmacol* 270(1):39–44
42. Kumar V, Tripathi VK, Singh AK, Lohani M, Kuddus M (2013) Trans-resveratrol restores the damages induced by organophosphate pesticide-monocrotophos in neuronal cells. *Toxicol Int* 20(1):48–55
43. Toth P, Tarantini S, Tucsek Z, Ashpole NM, Sosnowska D, Gautam T, Ballabh P, Koller A et al (2014) Resveratrol treatment rescues neurovascular coupling in aged mice: role of improved cerebrovascular endothelial function and downregulation of NADPH oxidase. *Am J Phys Heart Circ Phys* 306(3):H299–H308
44. Kashyap MP, Singh AK, Kumar V, Yadav DK, Khan F, Jahan S, Khanna VK, Yadav S et al (2012) Pkb/Akt1 mediates Wnt/GSK3 β / β -catenin signaling-induced apoptosis in human cord blood stem cells exposed to organophosphate pesticide monocrotophos. *Stem Cells Dev* 22(2):224–238
45. Kashyap M et al (2010) Caspase cascade regulated mitochondria mediated apoptosis in monocrotophos exposed PC12 cells. *Chem Res Toxicol* 23(11):1663–1672
46. Zhou X-M, Zhou ML, Zhang XS, Zhuang Z, Li T, Shi JX, Zhang X (2014) Resveratrol prevents neuronal apoptosis in an early brain injury model. *J Surg Res* 189(1):159–165